Macromolecules **1991,** *24,* 2203-2207

Gas-Induced Plasticization and the Permselectivity of Poly(tetrabromophenolphthalein terephthalate) to a Mixture of Carbon Dioxide and Methane

R. T. Chern* and C. N. Provan

Department of Chemical Engineering, North Carolina State University, Raleigh, North Carolina 27695-7905

Received July 2, 1990; Revised Manuscript Received October 30, 1990

ABSTRACT: A high glass transition temperature (T_g = 319 °C), rigid-chain polymer, poly(tetrabromophenolphthalein terephthalate) (TBrPPha-tere), was synthesized and characterized by IR, ^{1}H NMR, intrinsic viscosity, GPC, DSC, and density measurements. Its permeability to pure carbon dioxide, pure methane, pure ethane, and a mixture of carbon dioxide and methane (32.3 mol % CO_2) at 35 °C was investigated. Despite its rigid backbone, TBrPPha-tere's permeability to either pure carbon dioxide or pure ethane showed a minimum at ~10 atm when measured as a function of the gas pressure. The normalized diffusion coefficient, $D(c)/D(c{=}0)$, of ethane increased more than 60 times over a small concentration range (~3.5 wt %), reflecting the effects of "gas-induced plasticization". Moreover, the mixed-gas permeabilities of carbon dioxide were much less than the corresponding pure-gas values at the same partial pressures. There also was not an upturn in the mixed-gas CO_2 permeability when the partial pressure of carbon dioxide was raised up to 15 atm. In contrast, the mixed-gas permeability of methane increased with methane partial pressure and surpassed its pure-gas value at the same partial pressure. The limitations of models based on Fick's first law for describing these mixed-gas permeability data are also addressed.

Introduction

The gas permeabilities of glassy polymers at pressures up to ~20 atm are commonly observed to decrease with increasing gas pressure. However, exceptions to this general behavior have been reported from time to time in the literature. Cellulose acetate[1-5] is the most well-known membrane-forming glassy polymer, whose permeability increases or remains constant with an increase in gas pressure (except at very low pressures), regardless of the nature of the gas. A few other low-T_g (<150 °C) glassy polymers[6-8] have also been reported to exhibit similar behavior in their permeabilities to carbon dioxide. "Normally behaved" high-T_g polymers were also found to exhibit this upswing in permeability with gas pressure as the upstream pressure exceeded a certain limit.[9,10] Since the amount of sorbed gas increases with increasing gas pressure, these latter observations suggest that the upswing in permeability with pressure is intimately related to the gas concentration inside the polymer.

Several researchers have reported the effects of sorbed gas on the physical properties of glassy polymers. Wang et al.[11] exposed a polystyrene sample to carbon dioxide at pressures up to ~1000 atm and measured the tensile compliance in situ. They found that the data collected at different carbon dioxide pressures can be shifted to generate a master curve, similar to the well-known time–temperature superposition principle.[12] By fitting the shift factor to an equation similar to the WLF equation, they calculated the effective glass transition temperatures of polystyrene at different carbon dioxide pressures and temperatures. They found that between 0 and ~100 atm, the glass transition temperature was reduced dramatically due to the "plasticization" effects of sorbed carbon dioxide on polystyrene. The reduction in the effective T_g diminished greatly as the pressure was increased to higher than 100 atm, presumably because of the counteracting compaction effects attributed to the large hydrostatic pressure. At 34 and 45 °C, the relaxation modulus of polystyrene was also found to decrease by ~2 orders of magnitude before the hydrostatic pressure effects caused the modulus to rise from a minimum.

By heating in a DSC furnace thick samples, which have been preequilibrated at different carbon dioxide pressures, Chiou et al.[13] and Sanders[14] reported the T_g of several glassy polymers as a function of the sorbed carbon dioxide concentration. The magnitude of reduction in T_g appeared to be a unique function of the sorbed carbon dioxide concentration, independent of the nature of the glassy polymer. For example, at a sorbed carbon dioxide concentration of 40 cm^3 (STP)/cm^3 of polymer, the glass transition temperature dropped about 40–50 °C. In addition, the sorption isotherms for carbon dioxide in many low-T_g polymers were found to exhibit the typical "dual-mode" shape at low pressures but turn linear at higher pressures.[13] Chiou et al. interpreted the concave-to-linear transition to be the glass-to-rubber transition. The glass transition temperature determined this way was in reasonable agreement with that determined from the DSC method mentioned above.[13]

Conceivably, when the extent of plasticization is large, the effective gas diffusivity inside the polymer will show a remarkable upward dependency on the sorbed gas concentration, which then causes the upswing in permeability mentioned in the first paragraph.

In this paper, we present the synthesis, characterization, and permeability of a high-T_g rigid-chain glassy polymer, poly(tetrabromophenolphthalein terephthalate) (TBrPPha-tere), to several pure gases and a mixture of carbon dioxide and methane. Despite the high glass transition of TBrPPha-tere (319 °C), effects of the above-mentioned "gas-induced plasticization" are found to be quite dramatic.

Experimental Section

Chemicals. Triethylamine, 1,2-dichloroethane, benzene, and *n*-hexane were dried with calcium hydride and stored over molecular sieves. The terephthaloyl chloride was recrystallized from its *n*-hexane solution. All other chemicals were of the highest purity available and were used as received without further purification. The CO_2/CH_4 gas mixture composition was determined by a Varian gas chromatograph (GC), which was calibrated with several gas mixtures prepared in this laboratory.

Polymerization. The repeat unit of poly(3′,3″,5′,5″-tetrabromophenolphthalein terephthalate) (TBrPPha-tere) is shown in Figure 1. Low-temperature solution polymerization similar to that reported in a previous paper[15] was used. The resulting

0024-9297/91/2224-2203$02.50/0

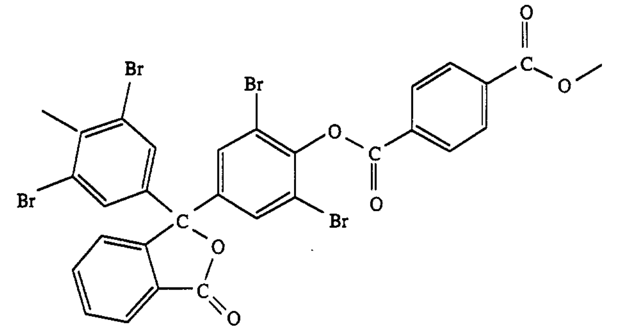

Figure 1. Repeat unit of TBrPPha-tere.

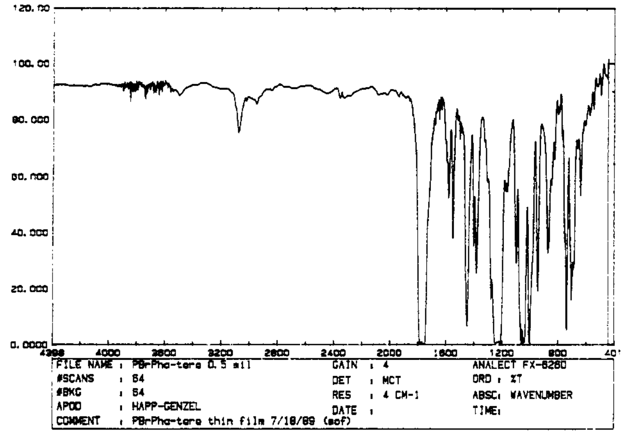

FILE NAME : PBrPha-tere 0.5 mil
#SCANS : 64
#BKG : 64
APOD : HAPP-GENZEL
COMMENT : PBrPha-tere thin film 7/18/89 (sof)
GAIN : 4
DET : MCT
RES : 4 CM-1
DATE :
ANALECT FX-6260
ORD : %T
ABSC: WAVENUMBER
TIME:

Figure 2. FTIR spectrum of TBrPPha-tere.

polymer was thoroughly purified by repeated dissolution, precipitation, washing, and drying before use.

Characterization. Solution viscosity measurements were made with a Cannon-Ubbelohde viscometer (standard size one) at 20 °C. The solvent used was 1,1,4,4-tetrachloroethane. Both the Huggins equation[16] and the Kraemer equation[17] were used to determine the intrinsic viscosity. Fingerprint analysis of the polymer was done with an Analect Fourier transform infrared spectrometer (FTIR) and a GE 300-MHz nuclear magnetic resonance spectrophotometer (NMR). The density of the polymer sample was determined at 23 °C with a density gradient column of aqueous zinc chloride solutions. The glass transition temperature (T_g) was determined with a Perkin-Elmer differential scanning calorimeter (DSC VII).

Sorption and Permeation. Steady-state permeability to pure gases and sorption isotherms of the pure gases were measured with established methods and will not be repeated here.[18-20] All the permeability data were determined with a 1.1 ± 0.1 mil (27.9 ± 2.5 μm) thick film that had been "vector-conditioned"[19,21] with CO_2 at 21 atm. The permeation area was 14.5 cm^2. All sorption isotherms reported here were determined after the polymer had been "conditioned" with CO_2 at 21 atm and 35 °C. The procedure used for analyzing the permeate compositions was different from those reported in the literature[22] and is presented in the Appendix.

Results and Discussion

Polymer Characterization. The intrinsic viscosity of the TBrPPha-tere sample was found to be 0.369 dL/g from both the specific viscosity and the inherent viscosity plots. The gel permeation chromatography (GPC) elution curve for the sample showed a single broad peak, and the $\bar{M}_w/\bar{M}_n$ ratio was estimated to be ~2 with an $\bar{M}_w$ of 26 000 based on calibration with polystyrene standards. The T_g of TBrPPha-tere is 319 °C according to the second DSC heating scan.

No carboxyl or hydroxyl groups are detectable in the IR spectrum of TBrPPha-tere (Figure 2). The ^{1}H NMR spectra are shown in parts a and b of Figure 3. In Figure 3b, tentative assignments of the various shifts are suggested. The shift at δ 4 (Figure 3a) is attributed to the hydrogens of methyl ester. Since methanol was used to terminate the polymerization reaction and to precipitate the polymer, it is expected to have reacted with the acid chloride residue to form the methyl ester end cap.

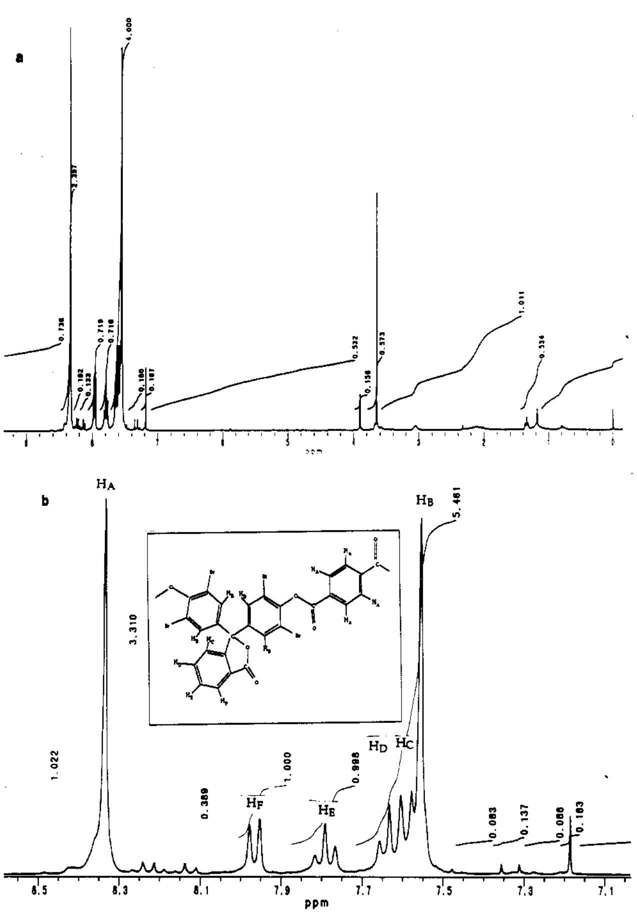

Figure 3. ^{1}H NMR spectrum of TBrPPha-tere.

The density of TBrPPha-tere determined by the density gradient column is 1.750 g/cm^3. A parameter, $1/V_f$, defined by $1/V_f = V/(V - V_{vw})$, has been demonstrated to be a useful index for ranking the packing density of polymers.[23] A larger $1/V_f$ corresponds to a denser packing. V is the measured specific volume of the polymer, and V_{vw} is the specific van der Waals volume calculated from the group contribution method developed by Bondi.[24]

The $1/V_f$ value of TBrPPha-tere is 2.66, smaller than its unbrominated counterpart, PPha-tere ($1/V_f = 2.78$).[23] This result is consistent with an earlier observation[25,26] that aryl bromination is effective in reducing the packing density of aromatic glassy polymers.

Steady-State Permeability and Plasticization. The permeabilities of TBrPPha-tere to carbon dioxide, methane, and ethane are plotted versus the upstream pressure in Figure 4. The ethane and carbon dioxide permeabilities both go through a minimum at around 10 atm of upstream gas pressure. In contrast, the methane permeability conforms to the normal "dual-mode" behavior; namely, it decreases with increasing pressure. The data for other gases are qualitatively similar to those of methane and will be omitted in most of the following discussion. These data can be found in a separate paper dealing with a different issue.[27]

Since the solubilities of different gases differ greatly, a more appropriate presentation is to plot permeability versus upstream gas concentration in the polymer, as shown in Figure 5. Clearly, gas concentration in the polymer is a major factor that contributes to the upturn in permeability. However, the nature of the gas molecules

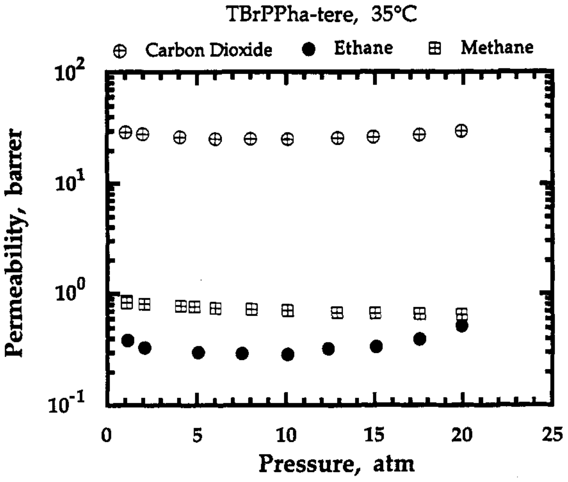

Figure 4. Permeability of TBrPPha-tere as a function of upstream pressure. 1 barrer = 10^{-10} cm^3 (STP)-cm/cm^2-s-cmHg.

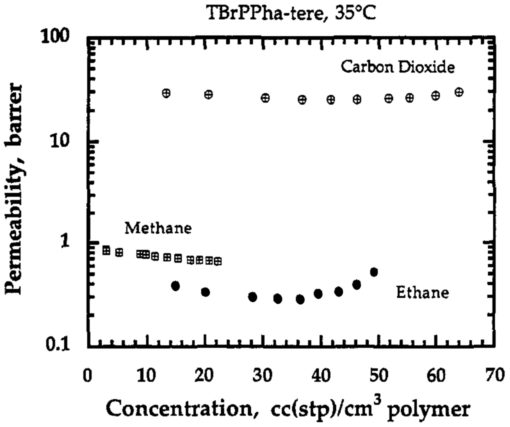

Figure 5. Permeability of TBrPPha-tere as a function of upstream sorbed gas concentration.

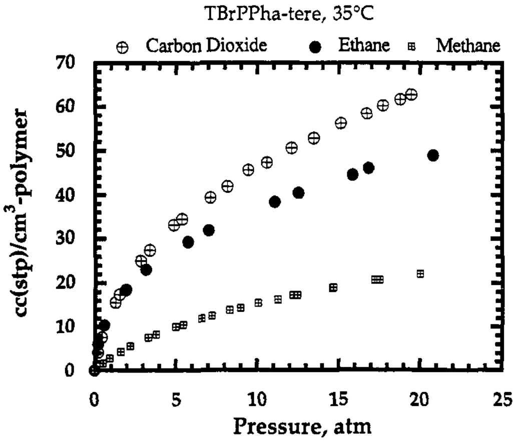

Figure 6. Equilibrium gas sorption isotherms for TBrPPha-tere.

also appears to be a significant factor, as reflected in the more dramatic pressure dependence of the ethane permeability.

The equilibrium sorption isotherms for all three gases (Figure 6) exhibit the shape typically observed for glassy polymers.[28] According to the interpretation of Chiou et al.,[13] the shape of these isotherms suggests that the glass transition temperature of TBrPPha-tere remained above 35 °C in the presence of the sorbed gases. Quantitatively, even when TBrPPh-tere absorbs 65 cm^3 (STP) of carbon dioxide/cm^3 of polymer, no more than 80 °C depression in T_g is expected from the equation developed by Chow.[29] The present findings clearly reinforce Sanders' proposition[14] that upturn in the permeability vs pressure plot is not due to the glass-to-rubber transition brought about by the sorbed gases.

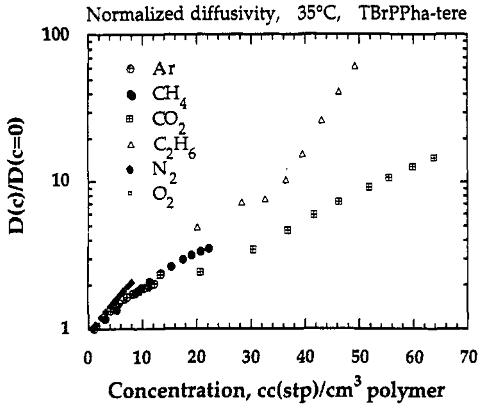

Figure 7. Concentration dependence of the normalized diffusion coefficient.

Assuming the validity of Fick's first law with a concentration-dependent diffusion coefficient, $D(c)$, applied to steady-state permeation with an approximately zero downstream pressure, one can derive the equation

$$D(c_2) = \left.\frac{d(N^{ss}l)}{dc}\right|_{c_2} \qquad (1)$$

where N^{ss} is the experimental steady-state flux, l is the thickness of the flat polymer film, and c_2 is the upstream gas concentration in the polymer. Equation 1 allows one to determine the effective diffusion coefficient as a function of concentration from experimental steady-state flux and equilibrium sorption data.[22] Using the dual-mode partial immobilization model,[30] we extrapolated the low-pressure data to estimate $D(c_2{=}0)$. The normalized effective diffusivity, D_{neff}, defined as $D(c_2)/D(c_2{=}0)$, is plotted versus concentration in Figure 7. Clearly, D_{neff} increases nearly exponentially over a wide range with the gas concentration in the polymer.

At low concentrations (e.g., <20 cm^3 (STP)/cm^3 of polymer), the curves for all the gases form a narrow band, suggesting that the nature of the gas molecules has little influence on the concentration dependence of the gas diffusivity. This is the range over which the concentration dependence of the diffusivity can be satisfactorily modeled and rationalized by the constant-diffusivity partial immobilization model.[22,30,31] However, at around 30–35 cm^3 (STP)/cm^3 of polymer, sharp increases in the D_{neff} values of CO_2 and C_2H_6 occurred, which exemplified the remarkable effects of gas-induced plasticization on the gas diffusivity. For example, the D_{neff} value for the larger size molecule, ethane, increases more than 60 times over the ~3.5 wt % concentration range covered. Why TBrPPha-tere exhibits such propensity toward gas-induced plasticization is an issue of continuing research in our laboratory.

Mixed-Gas Permeation. The mixed-gas permeation results are shown in parts a and b of Figure 8. The three data points at the lowest pressures were collected under different conditions and will be discussed in the Appendix. The other data points were collected when the upstream pressure was incrementally increased from ~15 to ~47 atm. To ensure that steady state had been reached, the polymer film was exposed to the feed gas for at least 3 days at each pressure.

Surprisingly, the mixed-gas CO_2 permeability decreased with increasing CO_2 partial pressure and was less than that of the pure gas over the same CO_2 partial pressure range. No upturn in the permeability was discernible at $P_{CO_2} > 10$ atm, in sharp contrast to the pure-gas behavior.

The mixed-gas CH_4 permeability was initially less than the pure-gas permeability and then rapidly increased at

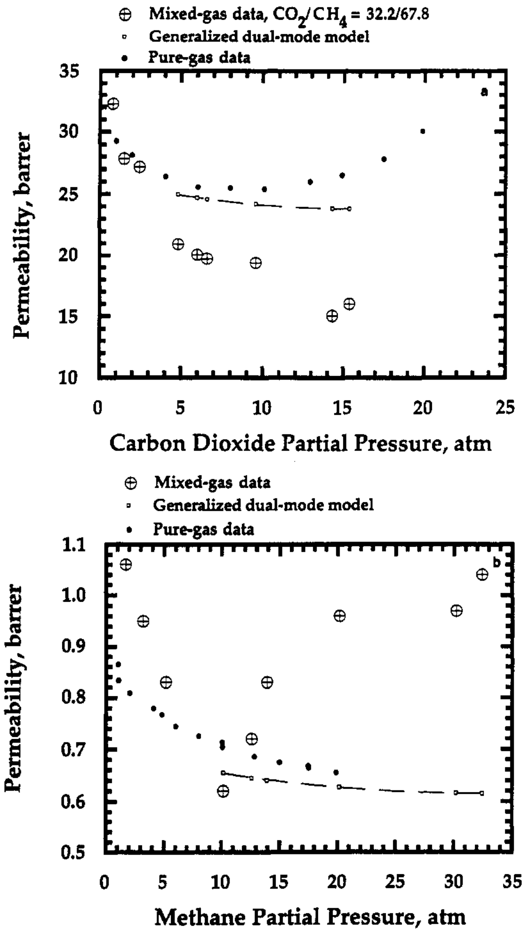

Figure 8. Mixed-gas permeability: (a) carbon dioxide, (b) methane.

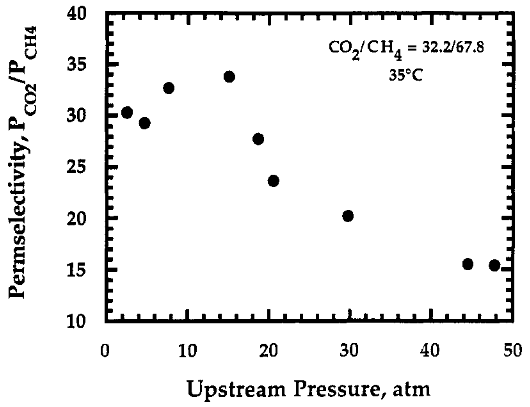

Figure 9. Intrinsic permselectivity of TBrPPha-tere for the CO_2/CH_4 mixture.

higher CH_4 partial pressures to larger than that for pure CH_4 over the same range of partial pressure. Correspondingly, the experimental permselectivity of TBrPPha-tere, defined as $\alpha \equiv P_{CO_2}/P_{CH_4}$, decreased dramatically with upstream total pressure as shown in Figure 9.

A generalized dual-mode partial immobilization model[32] had been developed for describing the mixed-gas permeability of glassy polymers. The model, with appropriate modifications to account for gas-phase nonideality,[22] was found to agree well with mixed-gas data for cases where no upturn was observed in the pure-gas permeability vs pressure plot.[22,33-35] However, the data in Figure 8 clearly cannot be fitted with this model in either the pressure or fugacity format.

Modification of the dual-mode model to allow description of the pure-gas permeability in the "plasticized" region has been reported.[36] The modification relaxes the assumption of constant diffusivity (in the original model) of the "dissolved" species and allows the diffusivity to increase with sorbed gas concentration. Obviously, this approach would describe the above CO_2 permeability data of TBrPPha-tere if the polymer sorbed less mixed gas (or CO_2, if one chooses to assume that CH_4 does not contribute to plasticization at all) than pure CO_2 at the same CO_2 partial pressure. However, if the mixed-gases data for PMMA[20] are of any guide, the above scenario is highly unlikely to happen.

The same analysis can be applied to any model that is based on the Fick's first law and a monotonic increase of diffusivity with sorbed gas concentration. Similar conclusions would be reached.

The above discussion thus suggests the presence of "multicomponent effects"; namely, the diffusional fluxes of carbon dioxide and methane are determined not only by their own respective concentration gradients but also by each other's concentration gradient.[37] The multicomponent effects became significant presumably because the permeating penetrants compete not only for limited sorption sites[32] but also for diffusion paths.

Additional evidence of multicomponent effects can be found in the literature. Cellulose acetate appears to be the only other glassy polymer whose carbon dioxide permeability increases with pressure and whose permeability to CO_2/CH_4 mixtures has been reported. The mixed-gas CO_2 permeability of cellulose acetate increased with pressure; however, it was less than the pure-gas value at the same CO_2 partial pressure, similar to what was observed with TBrPPha-tere. Again, a model without accounting for the multicomponent effects failed to describe the mixed-gas permeability data of cellulose acetate unless one assumes that the ability of either gas to cause plasticization depends on whether pure-gas or mixed-gas is used.[3]

Conclusions

TBrPPha-tere was shown to exhibit a reasonable permeability ($P_{CO_2} > 25$ barrers) and permselectivity (25–35) to a mixture of carbon dioxide and methane (32.2 mol % CO_2) at 35 °C and pressures less than 20 atm. Unexpectedly, this high-T_g, rigid-backbone polymer was susceptible to the effects of gas-induced plasticization. Large increases in the diffusion coefficients of both pure carbon dioxide and pure ethane were observed as the sorbed gas concentration exceeded roughly 30–35 cm^3 (STP)/cm^3 of polymer. Moreover, the mixed-gas carbon dioxide permeabilities were found to be much less than the pure-gas values although the mixed-gas methane permeabilities behaved as expected from the current understanding of gas-induced plasticization. Conceptual argument was presented to show that models not accounting for multicomponent effects are not likely to describe the depression in mixed-gas CO_2 permeability from its corresponding pure-gas values in the plasticization pressure range.

Acknowledgment. We are thankful to the donors of the Petroleum Research Fund, administered by the American Chemical Society, for support of this research. Fellowship to C.N.P. provided by the Plastic Institute of America is also highly appreciated.

Appendix

I. Mixed-Gas Permeability Measurement. These measurements were made with the same equipment as that used for pure-gas permeation except for a few

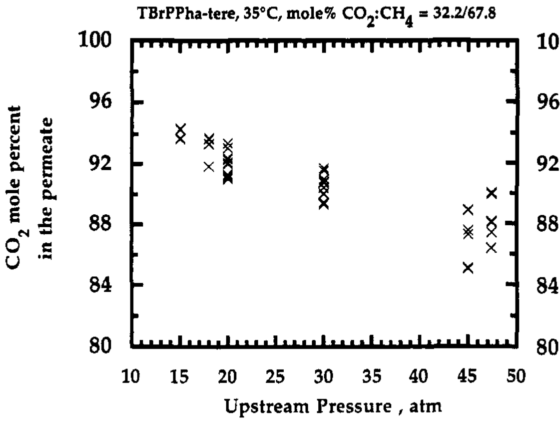

Figure 10. Reproducibility of the permeate composition analysis.

modifications to allow for downstream gas analysis and minimization of upstream concentration polarization. The high-pressure stream was fed continuously across the upstream surface of the polymer film, its flow rate was adjusted so that no more than 0.5% of the feed permeated through the film to the downstream side of the cell (i.e., stage cut <0.5%). The feed gas was passed through about 10 ft of $^1/_8$-in. stainless steel tubing in the thermostated permeation box so that the gas reached thermal equilibrium with the surroundings (35 °C) before coming in contact with the polymer film.

Downstream pressure–time data at small pressures (<10 Torr) were used for determining the permeation flux. However, the downstream pressure was allowed to increase to a maximum pressure of about 500 Torr in order to collect an adequate amount of sample for compositional analysis. A Perkin-Elmer Sigma 2000 gas chromatograph (GC) equipped with a thermal conductivity detector (TCD) was used for gas composition analysis. Argon was the carrier gas. Gas permeated through the polymer and was collected in a 50-cm^3 stainless steel reservoir, which was connected to the downstream side of the film and could be detached via a leak-proof quick-connector. After the reservoir was disconnected from the permeation system, its content was diluted with argon until the pressure in the reservoir reached about 1500 Torr. This pressurized gas was then connected to a gas sampling valve for injection.

The mixed-gas permeability was calculated from the flux of the individual components and the partial pressure. For example, the CO_2 permeability is calculated from

$$P_{CO_2} = \frac{N y_{CO_2} l}{\Delta p_{CO_2}} \tag{2}$$

where N is the steady-state flux of the gas mixture across the membrane, y_{CO_2} is the CO_2 mole fraction in the permeate, l is the membrane thickness, and Δp_{CO_2} is the partial pressure difference of CO_2 across the membrane.

Averages of multiple injections of the permeate were reported in Figure 8. The reproducibility of the GC analyses is illustrated in Figure 10. Obviously, the deviation of the mixed-gas values from the pure-gas values in Figure 8 far exceeds the experimental error.

II. Low-Pressure Mixed-Gas Permeability. Three more mixed-gas measurements were made at total pressures less than 10 atm after the study at 48 atm was completed. The feed pressure was reduced gradually to 2.5 atm. The polymer film was exposed to this low-pressure feed gas for more than 10 days before permeability measurement was made. These results correspond to the three data points at the lowest pressures in Figures 8–10. Koros et al. had shown that high CO_2 pressure "conditioning" followed by depressurization increased remarkably the permeability of a glassy polymer and decreased only slightly the permselectivity of the polymer.[38,39] The three low-pressure data in the present system apparently are consistent with their findings.

References and Notes

(1) Wensley, C. G.; Jakabhazy, S. Z. *AIChE Winter National Meeting*, 1984.
(2) Lee, S. Y.; Minhas, B. S.; Donohue, M. D. *AIChE Symp. Ser.* **1988**, *84*, 93.
(3) Donohue, M. D.; Minhas, B. S.; Lee, S. Y. *J. Membr. Sci.* **1989**, *42*, 197.
(4) Puleo, A. C.; Paul, D. R.; Kelley, S. S. *J. Membr. Sci.* **1989**, *47*, 301.
(5) Sada, E.; Kumazawa, H.; Xu, P.; Wang, S.-T. *J. Polym. Sci., Polym. Phys. Ed.* **1990**, *28*, 113.
(6) Chiou, J. S.; Paul, D. R. *J. Appl. Polym. Sci.* **1986**, *32*, 2879.
(7) Chiou, J. S.; Paul, D. R. *J. Membr. Sci.* **1989**, *45*, 167.
(8) Puleo, A. C.; Muruganandam, N.; Paul, D. R. *J. Polym. Sci., Polym. Phys. Ed.* **1989**, *27*, 2385.
(9) Chern, R. T. *Abstracts of Papers*, 197th National Meeting of the American Chemical Society, Dallas, TX, April 9–14, 1989; American Chemical Society: Washington, DC, 1989.
(10) Koros, W. J.; Hellums, M. W. *Fluid Phase Equilib.* **1989**, *53*, 339.
(11) Wang, W. J.; Kramer, E. J.; Sachse, W. H. *J. Polym. Sci., Polym. Phys. Ed.* **1982**, *20*, 1371.
(12) Ferry, J. D. *Viscoelastic Properties of Polymers*; Wiley: New York, 1961.
(13) Chiou, J. S.; Barlow, J. W.; Paul, D. R. *J. Appl. Polym. Sci.* **1985**, *30*, 2633.
(14) Sanders, E. S. *J. Membr. Sci.* **1988**, *37*, 63.
(15) Chern, R. T.; Brown, N. F. *Macromolecules* **1990**, *23*, 2370.
(16) Huggins, M. L. *J. Am. Chem. Soc.* **1942**, *64*, 2716.
(17) Kraemer, E. O. *Ind. Eng. Chem.* **1938**, *30*, 1200.
(18) Felder, R. M.; Huvard, G. S. *Methods of Experimental Physics*; Academic Press: New York, 1980; Vol. 16c, p 315.
(19) Provan, C. N. M.S. Thesis, North Carolina State University, 1990.
(20) Sanders, E. S.; Koros, W. J.; Hopfenberg, H. B.; Stannett, V. T. *J. Membr. Sci.* **1984**, *18*, 53.
(21) Wonders, A.; Paul, D. *J. Membr. Sci.* **1979**, *5*, 63.
(22) Chern, R. T.; Koros, W. J.; Yui, R.; Hopfenberg, H. B.; Stannett, V. T. *J. Polym. Sci., Polym. Phys. Ed.* **1984**, *22*, 1061.
(23) Chern, R. T. *Sep. Sci. Technol.*, in press.
(24) Bondi, A. *J. Phys. Chem.* **1964**, *68*, 441.
(25) Chern, R. T.; Sheu, F. R.; Jia, L.; Stannett, V. T.; Hopfenberg, H. B. *J. Membr. Sci.* **1987**, *35*, 103.
(26) Chern, R. T.; Jia, L.; Shimoda, S.; Hopfenberg, H. B. *J. Membr. Sci.* **1990**, *48*, 333.
(27) Chern, R. T.; Provan, C. N., accepted by *J. Membr. Sci.*
(28) Koros, W. J.; Chern, R. T. In *Handbook of Separation Process Technology*; Rousseau, R. W., Eds.; John Wiley & Sons: New York, 1987; Chapter 20.
(29) Chow, T. S. *Macromolecules* **1980**, *13*, 362.
(30) Paul, D. R.; Koros, W. J. *J. Polym. Sci., Polym. Phys. Ed.* **1976**, *14*, 675.
(31) Chern, R. T.; Koros, W. J.; Sanders, E. S.; Chen, S. H.; Hopfenberg, H. B. *Industrial Gas Separations*; ACS Symp. Ser. 223; Whyte, J. T. E., Yon, C. M., Wagener, E. H., Eds.; American Chemical Society: Washington, DC, 1983; p 47.
(32) Koros, W. J.; Chern, R. T.; Stannett, V. T.; Hopfenberg, H. B. *J. Polym. Sci., Polym. Phys. Ed.* **1981**, *19*, 1513.
(33) Chern, R. T.; Koros, W. J.; Hopfenberg, H. B.; Stannett, V. T. *J. Polym. Sci., Polym. Phys. Ed.* **1983**, *21*, 753.
(34) Barbari, T. A.; Koros, W. J.; Paul, D. R. *J. Membr. Sci.* **1989**, *42*, 69.
(35) Story, B. J.; Koros, W. J. *J. Polym. Sci., Polym. Phys. Ed.* **1989**, *27*, 1927.
(36) Zhou, S.; Stern, S. A. *J. Polym. Sci., Polym. Phys. Ed.* **1989**, *27*, 205.
(37) Cussler, E. L. *Multicomponent Diffusion*, 1st ed.; Elsevier: Amsterdam, The Netherlands, 1976.
(38) Jordan, S. M.; Koros, W. J.; Flemming, G. K. *J. Membr. Sci.* **1987**, *30*, 191.
(39) Jordan, S. M.; Koros, W. J.; Beasley, J. K. *J. Membr. Sci.* **1989**, *43*, 103.

Registry No. TBrPPha-tere (copolymer), 132802-07-4; TBrPPha-tere (SRU), 132775-39-4; CO_2, 124-38-9; CH_4, 74-82-8; CH_3CH_3, 74-84-0.